

CORRELATION OF UAV-BASED MULTISPECTRAL VEGETATION INDICES AND LEAF COLOR CHART OBSERVATIONS FOR NITROGEN CONCENTRATION ASSESSMENT ON RICE CROPS

C. M. Bacsa¹, R. M. Martorillas¹, L. P. Balicanta¹, A. M. Tamondong¹

¹Department of Geodetic Engineering, University of the Philippines – Diliman, Quezon City, Philippines - (cmbacsa, rmmartorillas, amtamondong, lpbalicanta)@up.edu.ph

Commission IV

KEY WORDS: Leaf Color Chart (LCC), Unmanned Aerial Vehicle (UAV), Nitrogen Monitoring, Fertilizer Application, Rice Crops, Vegetation Index (VI)

ABSTRACT:

Fertilizer application is a crucial farming operation for regulating crop health thus crop yield. Optimal fertilizing doubles agricultural production subsequently raising farmers' income, food security and economic agriproducts. To optimize the application of fertilizers, initial monitoring of the current nutrient status of the crops is required. This research will focus on Nitrogen (N), the most extensive fertilizer nutrient in crop cultivation. Conventional N monitoring involves the use of Leaf Color Charts (LCC) wherein leaf color intensity is associated with the N content of the crops. Despite its ability to quantify the optimal amount of needed fertilizers, the LCC method requires extensive on-site labor and lacks accuracy. This study developed a method that incorporates capabilities of Unmanned Aerial Vehicles (UAVs) equipped with a multispectral sensor in N monitoring specifically in rice crops, a major agricultural product in the Philippines. In situ N level information collected through LCC was correlated with remote sensing data, particularly vegetation indices (VIs) extracted from UAV multispectral imagery of a rice plantation in San Rafael, Bulacan. Several VIs sensitive to crop N content were tested to determine which has the highest correlation with the LCC data. Through Pearson correlation and regression analysis, NDVI_{Red Edge} was found to be the most strongly correlated with LCC data suggesting its potential in mapping variability in fertilizer requirements. An equation modelling LCC observations and NDVI_{Red Edge} values that estimates the N levels of an entire rice plantation was generated along with the N concentration map of the study area.

1. INTRODUCTION

1.1 Background of the Study

Nutrient management is an integral part of fertilizer application. Practical methods in balancing nutrients optimize crop yield, maintain soil health and reduce the chances of surface and ground water contamination. Optimizing fertilization involves monitoring the existing nutrient status of the present vegetation stage. The level and concentration of crop nutrients are initially assessed to quantify sufficient amounts of needed fertilizers.

Nitrogen (N) is a primary crop nutrient essential for rapid growth, grain yield and quality. Among the fertilizers used by local farmers, 39.4% of which are N-based making it the most commonly used nutrient in farming (Cruz P. S., 1997). These type of fertilizers, when applied at optimal amounts significantly increase agricultural output at low cost. However both excessive and deficient fertilizer application result to imbalances in the agricultural setting. Thus, the research industry continues to seek efficient ways for N management in farmlands. Through the collaboration of the International Rice and Research Institute (IRRI) and PhilRice, the Philippine agricultural sector adopted the use of Leaf Color Charts (LCCs). These are four-panel tools with varying shades of green conventionally used to determine leaf color intensity directly related to crop N level (Cruz & Obien, 1997). Similar to other conventional ground-based methods, the use of LCCs require extensive on-site labor and involves subjective measurements which are highly prone to inaccuracies. Several studies suggest the integration of these conventional methods with Unmanned Aerial Vehicle

(UAV) capabilities. Multispectral imagery captured by UAVs has been proven to be capable of providing information on crop conditions necessary for nutrient management. This study proposes a method that incorporates drone technology with the conventional LCC method to develop an efficient N monitoring scheme for optimal fertilizer application on rice plantations.

1.2 Research Objectives

This research aims to develop a method of crop N monitoring using remote sensing technology particularly UAVs. Primarily, the goal is the integration of a conventional ground-based farming practice, the LCC method, and drone technology. This study intends to provide a more accurate and modernized version of the LCC method through the incorporation of UAV imagery analysis. Through the correlation of LCC observations and parameters extracted from aerial imagery related to N content, a predictive model that estimates N levels of rice plantations will be generated. Specific objectives of the study include the assessment of N-sensitive Vegetation Indices (VIs) and the determination of the VI which is the most strongly correlated with LCC values. An equation modelling LCC readings and the best VI will be generated to predict the N levels throughout the study area. The output of this study is an N concentration map of a rice plantation in San Rafael, Bulacan. Such map aims to serve as guide for crop N management useful for fertilizer application. Furthermore, the outputs of this study may serve as supplementary information to assist agricultural sectors in implementing policies that will reduce fertilizer expenses and the adverse effects of N use in farming.

1.3 Significance of the Study

Conventional ground-based farming methods for N monitoring are often laborious and time consuming. Moreover, ground operations, if not costly, lack accuracy in measuring crop N levels. Farmers also deserve the convenience and benefits of technological advancements, thus, through the incorporation of UAV remote sensing, N monitoring may be made more convenient and efficient. This study assessed the capability of UAV imagery for N management. This integration of agriculture and remote sensing will allow farmers to manage crop's N level for optimal fertilization. Optimal fertilizing doubles agricultural production subsequently raising farmer's income, food security and economic agricultural products. This study envisions a system of N monitoring which will significantly raise agricultural output. This study proposes a method of using UAVs that could be a potential long term investment for agricultural municipalities to centralize N monitoring covering plantations within the municipality's boundaries.

1.4 Related Literature

Crop N monitoring is an essential requisite for optimizing fertilizer management. Through an efficient assessment of the current N status, required fertilizer inputs can be quantified to meet the sufficient nutrient requirement of crops without compensating the environment (Rochester, et al., 2009). Conventional methods include the actual on-site field observations using leaf sampling for laboratory analysis and chlorophyll level inspection through visual inspection of leaf greenness index. However, these procedures exhibit restrictions including time, productivity and cost. In acknowledgment of this, recent technological advancements showed an increase in the use of UAV capabilities in precision agriculture. As compared to satellites and other spaceborne platforms which requires scheduled overpass, a low-cost UAV allows time flexible data acquisition at a higher resolution.

Agricultural sectors have been widely utilizing UAVs for convenience and efficiency in drought stress detection, yield prediction and nutrient status assessment (Maes & Steppe, 2018). In particular, several studies has been suggesting the potential of drone and multispectral sensor integration in estimating crop N levels. Pölönen (2013) demonstrated image-based crop biomass and N content estimations through imagery acquired from a sensor mounted on a light-weight UAV. VIs extracted from the imagery were correlated with biomass and N content (Pölönen, 2013). Liu (2018) conducted a study on a winter oilseed rape farm and used optimal VIs from in situ hyperspectral data along with multispectral UAV imagery to estimate the crops' N nutrition index (NNI). Results of the study showed that among the tested VIs, the Normalized Difference VI (NDVI), Modified Soil-Adjusted VI 2 (MSAVI2) and Red Edge Chlorophyll Index ($CI_{Red\ Edge}$) showed the most accurate NNI estimations (Liu, et al., 2018). Pagola (2009) incorporated digital color image analysis on the estimation of crop N status. Correlation between VIs and Soil and Plant Analysis Development (SPAD) measurements were calculated proving the potential of VIs to predict N deficiencies (Pagola, et al., 2009).

Walsh, et al. (2018) assessed the N concentration level of a rice crop field through determining the most appropriate

vegetation index (VI) extracted from UAV imagery. In the same study, the study area was grouped into test and training data sets. Statistical analysis was performed to determine the R^2 and RMSE to evaluate each model equation. The study proved that remotely sensed VIs can provide valuable information on Nitrogen status (Walsh, et al., 2018). The methodology and parameters used for this research from the data acquisition up to the final map generation were all based from related studies regarding N monitoring using UAV imagery analysis.

2. METHODOLOGY

2.1 Field Visits and Planning

Consultation with research advisers and experts in the field of agriculture guided the methodological framework. Different factors that may affect the study were considered such as the study area and crop to be assessed, instruments and software availability, and the available budget to be used throughout the study. Through the Agricultural Municipal Office of San Rafael, Bulacan request for site access on a rice plantation was granted. Site inspection of the rice fields situated in Brgy. Caingin was done under the supervision of the municipal's agricultural technologist.

2.2 Study Area

The study area is a specific agricultural site situated in Barangay Caingin, San Rafael, Bulacan. The chosen region is specifically a rice crop plantation encompassing an approximate area of four (4) hectares. The area comprises of three (3) farmlands with varying fertilizer management practices particularly in terms of types and quantities of N-based fertilizers. The rice by the time of data acquisition were medium early maturing variety crops. The crops are at their active tillering stage which means that they have been cultivated for 24-28 days.

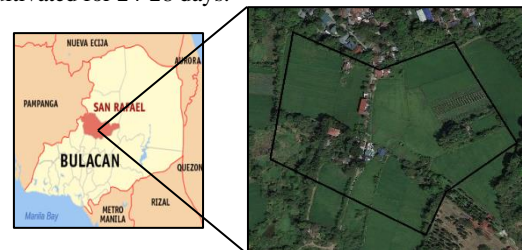


Figure 1. Delineation of Study Area in San Rafael, Bulacan



Figure 2. Rice Plantation Documentation

2.3 Flight Planning

Before the actual UAV employment, necessary flight parameters were set through flight planning and design. The flight path of the UAV covering the desired area was established by mission planning using the eMotion software. Wind condition, climate, obstructions, and other regions of high risk were taken into account. The final flight altitude

used in the operation on the region of interest was 74.3 m generating an output ground spatial distance resolution of 7.0 cm. The total flight area covered approximately eleven (11) hectares. Three (3) ground control points were established situated outside the study area boundary.

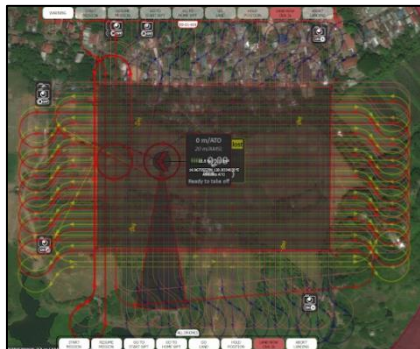


Figure 3. Flight path represented in red lines

2.4 Instruments

2.4.1 Parrot Sequoia

Parrot Sequoia has been proving the worth of its existence in the field of agriculture. This commercial sensor allows absolute reflectance measurements even without the use of reflectance targets. In this study, this multispectral sensor was used to monitor crop N status for optimization of fertilizer strategies to improve overall farm productivity. It is a 28 x 41 x 59 mm unit weighing 107 grams. It captures four different bands (Red, Green, Red Edge and Near Infrared) and has an additional 16 megapixel RGB camera. Parrot Sequoia comes with a sunshine sensor that records light conditions in the same spectral bands as the multispectral sensor. It records the irradiance for each image in each band and allows the normalization of the varying illumination during the data acquisition. Moreover, the sunshine sensor enables GPS data recording. Together, the two sensors obtain the true value of light and location at any given period. This unit was acquired through Envisage under the Department of Geodetic Engineering, University of the Philippines Diliman.

2.4.2 Sensefly eBee

For the image acquisition, the UAV used in the study was Sensefly eBee, a fixed wing drone, mounted with a Sequoia multispectral sensor. This is a fully autonomous mapping drone suited for various agricultural purposes. This unit weighing 700 grams can cover a maximum area of 1200 ha in a single automated mapping flight. The system includes batteries, an RGB camera, radio modem and an eMotion software. This drone enables the acquisition of high resolution imagery which can be further transformed into orthomosaic and 3d maps.

2.5 Data Acquisition

2.5.1 Ground Control Point (GCP) Establishment

Three (3) GNSS receivers were stationed on the field using a range pole and bipod setup. The tip of the metal shoe of the range pole was positioned at the center of the GCP marker. The bipod's legs were adjusted until the setup was stable.

The receiver was then mounted on the pole. The receiver and controller were connected via Bluetooth prior to the actual fieldwork. Local coordinates were used in the study. Using the Trimble controller, parameters and configurations were changed to make use of Post Process Kinematic (PPK) as survey style. Locations where recorded using the GPS controller simultaneously with the LCC observations. The exported file from the receiver were processed using the Trimble Business Center (TBC).



Figure 4. Setting up the GNSS Receiver (left) and actual target on GCP (right)

2.5.2 UAV Multispectral Imagery Acquisition

The project site was inspected to find an optimal location for the drone launching. An open space with less obstruction and low risk was chosen. Relative humidity and wind situation were taken into account. Upon finish of the GPS observations on each GCP, multispectral image acquisition using the fixed wing drone was performed. Imagery of the rice crop plantation was obtained through the equipped multispectral sensor. The drone was employed by a licensed pilot in autonomous mode. A total of three (3) flights with high overlap was executed by the drone to cover the study area.

2.6 In Situ N Level Data Collection

In obtaining ground values for N content, the conventional method of determining the N status of crops using an LCC was used. A total of twenty-two (22) sampling portions randomly placed on the field were established. Each sampling portion encompasses an area of 1 square meter. The coordinates of each corner of the plot was obtained using GNSS PPK and was recorded. For every plot, ten (10) healthy plants were selected. The topmost, fully-expanded and healthy leaf of each of the ten (10) plants was compared to the leaf color chart to assess the level of N content. When observing, the LCC was made sure to not be exposed to direct sunlight. Only one researcher examined and took LCC readings from the first to the last plot. The LCC used was acquired from the municipal agriculture office of San Rafael Bulacan.



Figure 5. Stakes for marking sampling quadrants (left) and LCC measurement (right)

As part of the validation process, leaf samples from two (2) quadrants on the field were obtained. A total of two (2) kilograms of leaf samples was gathered and submitted to the Plant Tissue Analysis Laboratory of the Philippine Coconut Authority. The samples were limited to two quadrants to comply with the allowed kilogram of plants to be obtained in the farm. Leaf sample collection is destructive for the crops thus it was greatly reduced.

2.7 Data Processing

2.7.1 GNSS Data Processing

The data acquired from the Static GNSS survey was processed in TBC. Necessary parameters including antenna height was fixed to 2.00 meters. Upon processing and adjustment of the network, the processed data containing the coordinates of the GCPs was exported. Same method was done to extract the coordinates of the sampling quadrant corners from the Kinematic dataset.

2.7.2 Image Post-processing

Multispectral image sets from the first and third flights were processed in Pix4Dmapper Pro. All 2780 images were geolocated with output coordinate system auto detected to be WGS84/ UTM zone 51N. The processing option used was Ag Multispectral, a template that uses sensors in a camera to generate radiometrically calibrated reflectance index, classification, and application maps for precision agriculture. The compatible cameras for AG Multispectral include Parrot Sequoia, Micasense Red Edge, and Airinov multiSPEC. For this study, Parrot Sequoia was used as the multispectral sensor. The final output are the reflectance tiles for each band (green, red, red edge and NIR). These reflectance tiles were used in the generation of the vegetation index maps.

2.7.3 GCP Application for Precise Image Positioning

After initial processing, GCPs were marked in the rayCloud of images. The adjusted coordinates exported from the Static Data Processing were used as GCPs for post-processing the multispectral imagery. Exact locations of GCPs on the image were marked. At least two (2) marked images were done to enable automatic marking of the GCPs. The software automatically selected the location of the GCP on every image through color correlation of the marked pixel on the rest of the images. Upon marking all GCPs on the image set, the processing was reoptimized.

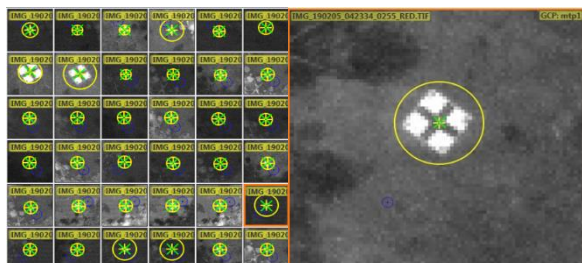


Figure 6. GCP marking in rayCloud view Pix4D

2.7.4 Generation of Vegetation Index Maps

Post-processed multispectral images were used to generate the VI maps processed using ArcMap 10.3. Image tiles having the same band were mosaicked to create a full band

image. Using combinations of these mosaicked images (Red, Red Edge, Green, and NIR), VI maps were generated using a raster calculator. This tool builds and executes an expression using a Python syntax in a calculator-like interface. Mathematical formulas for each VI sensitive to N content (CI_{Green}, CI_{Red Edge}, MTCI, NDVI, NDVI_{Red Edge}, and RTVI_{Core}) were based from Walsh, et.al (2018).

VI	NAME	FORMULA
CI _{Green}	Green Chlorophyll Index	(NIR/Green) – 1
CI _{Red Edge}	Red Edge Chlorophyll Index	(NIR/Red Edge) – 1
MTCI	Medium Resolution Imaging Spectrometer (MERIS) Terrestrial Chlorophyll Index	(NIR – Red Edge) / (Red Edge + Red)
NDVI	Normalized Difference Vegetation Index	(NIR – Red) / (NIR + Red)
NDVI _{Red Edge}	Red Edge Normalized Difference Vegetation Index	(NIR – Red Edge) / (NIR + Red Edge)
RTVI _{Core}	Core Red Edge Triangular Vegetation Index	100(NIR – Red Edge) – 10(NIR – Green)

Table 1. Vegetation Indices sensitive to crop Nitrogen

Feature polygons representing the sampling quadrants in the field were established and was overlaid in each VI map. These features were created using the Northings and Eastings of the corners obtained by GNSS. The mean VI for each of the twenty-two (22) quadrants were extracted using Zonal Statistics.

2.8 Statistical Analysis

2.8.1 Pearson Correlation

Pearson correlation was used to determine the best VI which has the strongest correlation with LCC value. Generally, the strength of correlation between remote sensing data and in situ ground data was determined by calculating the correlation coefficient (r). The VI and LCC values were treated as the independent (x) and dependent (y) variables respectively. The mathematical formula for computing r is shown in equation 1. The variable n represents the total sample population. The VI with the highest r value was chosen to generate the final model equation.

$$r = \frac{n \sum xy - (\sum x)(\sum y)}{\sqrt{n \sum (x^2) - (\sum x)^2} \sqrt{n \sum (y^2) - (\sum y)^2}} \quad (1)$$

2.8.2 Regression Analysis

Upon determining the VI with the highest correlation with LCC values, regression analysis was performed. Regression was done to find the line of best fit for the two sets of data, VI and LCC datasets. This is the most commonly used modeling method. Mathematical trend lines including linear, exponential, logarithmic, polynomial and power equations were fitted with the data. The trend line and its respective equation, which exhibited the best fit and obtained the highest coefficient of determination (r^2) was used as the final model. This model shall predict LCC values representing Nitrogen concentration levels using the best vegetation index.

2.8.3 Leave One-Out Cross-Validation

Leave-one-out cross-validation (LOOCV) was used to assess the performance of the model equation. This model validation technique measures how accurate the predictive model is. In LOOCV, the dataset was divided into training and test sets. Each iteration excluded one observation to be the test set, all the remaining belonged to the training set and was used to generate a model equation. The model tested the excluded observation. The root mean squared error (RMSE) for each iteration was computed and averaged to determine the coefficient of variation (CV). The lower the value of the CV, the more precise the estimate is. The formula for RMSE is shown in Equation 2. The variable n is the total sample population.

$$RMSE = \sqrt{\frac{\sum_{i=1}^n (Predicted_i - Actual_i)^2}{n}} \quad (2)$$

2.9 Generation of Nitrogen Concentration Map

The resulting model equation from the best relationship fit between the LCC observations and UAV-based VI was used to generate the N concentration map. After processing, mean values of VIs for each quadrant were recalculated using for quantitative validation. The resulting map showed the LCC levels throughout the study area which represents the N concentration level.

3. RESULTS AND DISCUSSION

3.1 LCC Observations and Laboratory Results

A total of twenty-two (22) sampling plots were observed from the three farmlands comprising the study area (Farms A, B, and C). Based from the Philippine Rice Research Institute (PhilRice) guidelines regarding the use of LCC, if most of the LCC readings are 4 and 5, then the plot where the LCC observations were obtained have sufficient Nitrogen level while those plots with mostly 2 and 3 readings have Nitrogen deficiency. A 30kg N/ha of fertilizer must be applied during dry season and 23 kg N/ha during the wet season.

Since the study area is not an experimental field, obtaining 1 kg of leaf samples on each sampling quadrant is impossible because it may affect the health of the rice crops. Hence, the 2 sets of leaf samples were gathered randomly from Farms A and B only and submitted to the laboratory. According to Munson (1998) the nitrogen concentration in plant tissue is deficient (if less than 2.50%), sufficient (if 2.50% to 4.50%) and excessive (if greater than 6.00%) (Munson, 1998).

Farm	LCC Observation	Laboratory Result
Farm A	3.91	2.761
Farm B	2.86	1.921

Table 2. Summary of Nitrogen Level in Farms A and B

Table 1 shows the summary of N level in Farms A and B. Following the PhilRice guidelines on using the LCC, the sampling quadrants in Farm A have sufficient N level while Farm B has N deficiency. From the laboratory analysis using UV-Vis Spectrophotometry, Farm A with 2.761% N total has sufficient nitrogen level while Farm B with 1.921% N total

is deficient in N level. The results from the two different methods of N assessment are comparable. The average values of the LCC observations in both farms are relative to the laboratory result.

3.2 GNSS Data Processing

This study doesn't involve global coverage and is not concerned with the position relative to a datum, thus Local Positioning System (LPS) was used during the fieldwork. Problems encountered during the GPS data processing include error in the network adjustment due to cycle slips. The discontinuity in the receiver's phase lock was fixed by editing the data manually. Table 2 shows the adjusted grid coordinates used for the GCP marking in the image post-processing.

GCP	Easting (m)	Easting Error	Northing (m)	Northing Error
1	277636.91	0.001	1655670.25	0.000
2	277613.53	0.001	1655782.74	0.001
3	277804.48	-----	1655610.28	-----

Table 3. Adjusted GCP grid coordinates

3.3 Sampling Quadrants

The coordinates from the exported PPK file served as the corners of the sample quadrants where the LCC observations were obtained. The northings and eastings data were used to create polygons in ArcMap 10.3 representing the sampling quadrants in the map. Figure 7 shows the distribution of sampling quadrants in Farms A and B plotted in the mosaicked Red Edge band imagery. Farm A has 11 sample points while Farm B has 9 sample points. The LCC readings were mostly obtained near the embankment between the rice fields since it is the most accessible area for observation.

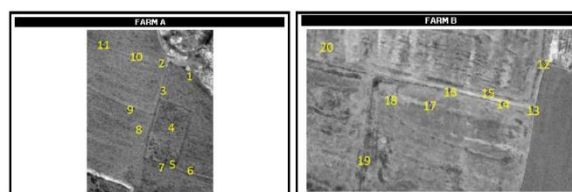


Figure 7. Sampling quadrants in Farm A and B

3.4 Image Post-processing Quality Report

The Ag Multispectral template in Pix4D Mapper was used to process the flights to generate the reflectance tiles per band. Upon completion of the post-processing method, a quality report (shown in Table 4) assessing the output images was generated.

Images	Median of 6362 keypoints per image
Dataset	2696 out of 2780 images calibrated
Camera Optimization	0.02% relative difference between initial and optimized internal camera parameters
Matching	Median of 1363.72 matches per calibrated image
Georeferencing	No 3D GCPs

Table 4. Image quality specifications

All 2804 images from flights 1 and 3 are geolocated. Since the number of keypoints is less than 10000, this suggests that less visual content could be extracted from the images.

Camera parameters such as shutter speed and exposure time should be adjusted. This variable however has a small impact on the overall analysis since the study does not dwell on visual inspection but on the actual pixel information to be extracted. 96% of all images are calibrated in a single block. The difference between the initial and optimized internal camera parameters is 0.02%. This falls under the 5% standard for relative difference of the optimized value. A median of more than 1000 matches in this case 1363.72 denotes that the results in the calibrated regions are likely to be of best quality

The reflectance tiles (red, green, red edge, NIR) generated after processing demonstrated good quality specifications denoting reliability for further analysis.

3.5 Vegetation Index Maps

The Parrot Sequoia multispectral sensor used in the study captured four (4) discrete spectral bands: Red, Green, NIR, and Red Edge. Figure 8 shows the mosaicked images of the four bands. These mosaicked images were used to generate the vegetation index maps (shown in figure 9).

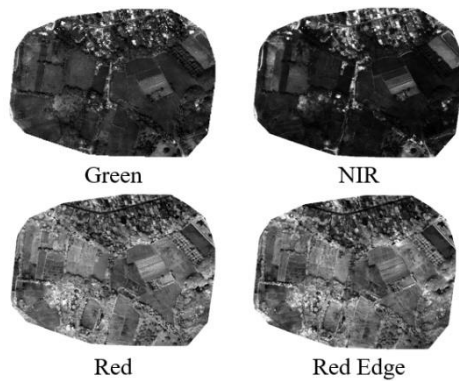


Figure 8. Mosaicked tile images per band

Subsequently, the mosaicked images were used to generate the vegetation index maps. The N-sensitive VI maps shown in figure 9 were created as mathematical combinations of the different mosaicked image bands. By visual inspection, the output VI maps vary from each other. No VI performed the same since each is a different combination of various multispectral bands.

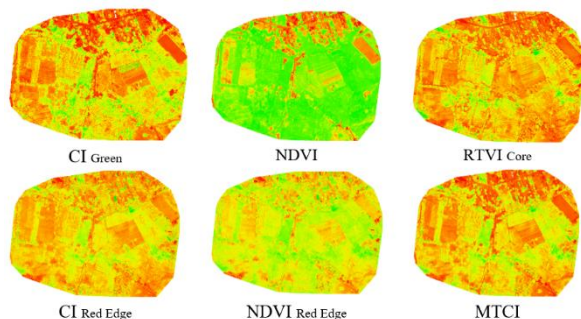


Figure 9. Vegetation Index Maps

3.6 Zonal Statistics

Upon generation of all necessary VI maps, the mean VI (CI Green, CI Red Edge, MTCI, NDVI, NDVI Red Edge, and RTVI Core) for each quadrant was extracted using the ArcMap zonal

statistics tool. The range of mean values for each vegetation index is shown in table 5.

Quadrant	MEAN VEGETATION INDICES					
	NDVI	NDVI Red Edge	CI Green	CI Red Edge	MTCI	RTVI Core
1	0.9041803	0.491228347	7.155611318	1.940497644	1.69305623	0.035770373
2	0.860881502	0.383746328	5.635734845	1.253392814	1.07513144	0.027345609
3	0.892083901	0.408389988	6.197055744	1.385401152	1.221776438	0.028426408
4	0.824118092	0.391564055	4.481306929	1.289884722	1.060396142	0.018522038
5	0.82594295	0.378517588	4.439473417	1.21045699	1.002689893	0.018726709
6	0.848670192	0.381351022	4.68999574	1.234404769	1.043819634	0.019999592
7	0.90263726	0.42060522	6.666526505	1.456064724	1.29578069	0.027402085
8	0.907417061	0.415929935	6.981679797	1.425986233	1.276475233	0.029808133
9	0.835297781	0.345864954	4.530771527	1.060946784	0.898116163	0.019646196
10	0.879767538	0.399492783	5.751229255	1.33533812	1.16660989	0.02856289
11	0.865094872	0.3841771	5.225109014	1.251283997	1.07926686	0.024433795
12	0.832561032	0.36376429	4.52739108	1.150705372	0.97071222	0.027946975
13	0.809296959	0.350816525	3.828281565	1.086803673	0.897108445	0.026400933
14	0.832867594	0.334285341	3.852162692	1.008095252	0.85450169	0.025178762
15	0.819857834	0.311536915	3.462135369	0.906579404	0.763412521	0.01979826
16	0.840342976	0.344780416	4.016566496	1.05553583	0.900252251	0.026149706
17	0.859640626	0.365846321	4.367290721	1.155107776	0.993807911	0.029454887
18	0.81776153	0.317942327	3.492433935	0.935573011	0.787272335	0.024007849
19	0.796154327	0.329182955	3.199132821	0.982936902	0.802748681	0.020147877
20	0.737451488	0.278716241	2.337588297	0.773745314	0.610794732	0.015975614
21	0.686324036	0.388129819	2.473153847	1.271742173	0.896948617	0.017603596
22	0.672561937	0.373153294	2.249035513	1.192457937	0.835654343	0.016796931

Table 5. Mean Vegetation Indices

Each VI exhibits a certain range of values. The NDVI values ranged from 0.6 to 0.9 which are values close to 1. This suggests that the regions where the VIs were extracted are areas of vegetation which holds true since the quadrants were established within the plantation. The NDVI Red Edge provides better measurements for latter stage crops since it can measure further down into the plant canopy. The values range from 0.27 to 0.49 which falls within the standard range for green vegetation for NDVI Red Edge. The Chlorophyll Index (CI) is used to calculate the chlorophyll content in leaves. The values of these indices are sensitive to even the slightest variations in chlorophyll content. The mean VIs for CI Green falls within 2.25 to 7.16 while CI Red Edge ranged from 0.77 to 1.94. The MTCI is a VI highly sensitive to chlorophyll concentration since reflectance values from NIR, Red and Red Edge bands were used in the calculation. The mean index values for each quadrant ranged from 0.61 to 1.69. The RTVI Core is another index that incorporated the reflectance values of the red edge band. The VI values for RTVI Core are relatively smaller than the other VIs.

3.7 Statistical Analysis

3.7.1 Pearson Correlation of LCC and VI datasets.

Pearson correlation was used to determine the VI which has the strongest correlation with in situ data for N concentration. The correlation coefficient between the VI and the LCC datasets were calculated to measure the degree of relationship between the two variables. Figure 10 shows the correlation coefficients (r) visualized as scatter plots. Among the VIs, NDVI Red Edge exhibited the strongest correlation with LCC observations with an r equal to 0.97.

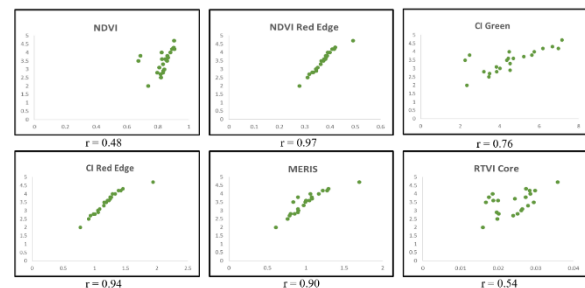


Figure 10. Pearson correlation visualized as scatter plot

3.7.2 Regression Analysis

Regression analysis was performed to determine the line of best fit with the NDVI_{Red Edge} values (independent variable) and the LCC values (dependent variable). Different trend lines including linear, exponential, logarithmic, polynomial and power were fitted to obtain the equation that will model the LCC and NDVI_{Red Edge} values. The whole datasets for both dependent and independent variables were used to generate the final model. The coefficient of determination (R^2) was also determined per best fit line. A high value of R^2 indicates that one variable is highly predictable from the other variable. The polynomial equation obtained the highest R^2 value of 0.9731 therefore, this was used as the final model equation for estimating LCC levels.

NDVI Red Edge		
Trendline	Equation	R^2
Linear	$y = 14.536x - 1.9352$	0.9431
Exponential	$y = 0.6628e^{4.4001x}$	0.9089
Logarithmic	$y = 5.4637\ln(x) + 8.9132$	0.964
Polynomial	$y = -35.312x^2 + 41.362x - 6.9594$	0.9731
Power	$y = 18.011x^{1.6723}$	0.9499

Table 6. Regression equations

3.7.3 Leave One-Out Cross-Validation

Using LOOCV, the performance of the final model equation was tested. LOOCV involves the calculation of RMSE per iteration. This was used to compute for the coefficient of variation (CV). The CV was computed to be 0.03, in statistics, a $CV < 1$ indicates low variance thus the generated equation is suggestive of a good model fit. Estimates that will be predicted by the model are precise and reliable.

$$LCC = -35.312 (NDVI_{Red Edge})^2 + 41.362 (NDVI_{Red Edge}) - 6.9594 \quad (3)$$

3.8 Nitrogen Concentration Map

Using the final model equation in (3), the N concentration map for the surveyed rice plantation in San Rafael, Bulacan dated February 5, 2019 was generated. Non-vegetation pixels were masked. The output map shows the corresponding predicted LCC values throughout the area. Interpreting this, portions exhibiting LCC 2 and LCC 3 indicates Nitrogen deficiency. According to the PhilRice guidelines, a 30 kg/ha of Nitrogen must be applied to these areas. Portions with LCC 4 and LCC 5 values denote sufficient Nitrogen levels.

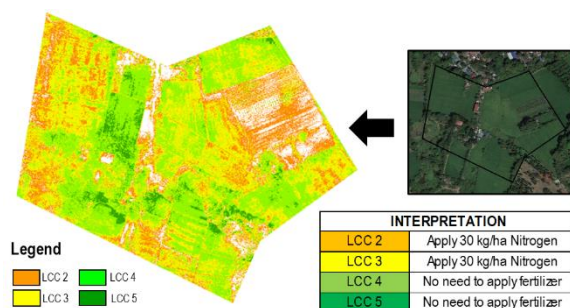


Figure 11. Nitrogen concentration map and corresponding fertilizer quantities according to PhilRice

4. CONCLUSION AND RECOMMENDATIONS

4.1 Conclusion

Integration of agriculture and remote sensing by UAV technology is a potential strategy for boosting agricultural output. Through efficient Nitrogen monitoring, fertilizer application may be optimized. This study proved an existing correlation between ground-based Nitrogen data obtained through Leaf Color Chart (LCC) observations with parameters extracted from drone imagery. Specifically, vegetation indices (VIs) acquired from the drone image processing were assessed to see the VI which is the most highly correlated with the LCC dataset. Primarily, the results of the study showed the possibility of using UAV-based Nitrogen sensitive VIs to quantify actual crop Nitrogen content in an evidently more efficient and reliable way as compared to most existing Nitrogen monitoring methods.

UAV integrated with a multispectral sensor having four discrete spectral bands (Green, Red, NIR, and Red Edge) is a promising technology specifically for precision agriculture. It was proved that UAVs are good aerial platforms for Nitrogen monitoring and a multispectral sensor is highly suitable for the determination of crop nutrient status. The methodology used for the assessment of Nitrogen concentration of rice crops in Farms A and B was ideal to reduce the detrimental effects of high levels of Nitrogen on the environment at the same time increase the economic yield of farmers. Lastly, the study is an advantage for large-scale Nitrogen monitoring. The method proposed in this research could be a long-term investment for agricultural municipalities to centralize Nitrogen monitoring covering all plantations within its boundary.

Upon the assessment of the six vegetation indices, NDVI_{Red Edge} had the highest correlation with the LCC observations. This denotes NDVI_{Red Edge} is a better indicator of Nitrogen level. This study proved findings on related literature suggesting that NDVI_{Red Edge} is the best VI to use when mapping variability in fertilizer requirements. The Nitrogen concentration map of a rice farm was generated from the best fit model equation along with the corresponding interpretation regarding the amount of needed fertilizer per portion. The output map showed its potential as reference for efficient Nitrogen management.

4.2 Recommendations

Since NDVI_{Red Edge} had the highest correlation with the LCC dataset, it is recommended to use a sensor with red edge band. In addition, LCC observations must be obtained in the morning, 8:00 – 10:00 AM, to avoid inaccuracies since the sunlight's glare affects the reflectance on the leaf samples. Moreover, LCCs must be measured in several sampling quadrants for sufficient training and test datasets. To have better validation, leaf samples must be gathered from the sampling quadrants where the LCC readings were obtained. However, due to its destructive effect, experimental fields must be used as study area. Other major agricultural crops such as corn and sugarcane may be explored and used as subject crops. Furthermore, the rice plantation used as study area only involved crops in their active tillering stage. Further studies may incorporate the growth stage and varieties of the subject crop as model variables.

REFERENCES

- Cruz, P. S. (1997). *Aquaculture Feed and Fertilizer Resources Atlas of the Philippines*. Food and Agriculture Organization of the United Nations.
- Cruz, R., & Obien, S. (1997). Leaf Color Chart. *Rice Technology Bulletin*.
- Liu, S., Li, L., Gao, W., Zhang, Y., Liu, Y., Wang, S., & Lu, J. (2018). Diagnosis of Nitrogen Status in Winter Oilseed Rape (*Brassica napus* L.) Using in-situ Hyperspectral Data and Unmanned Aerial Vehicle (UAV) Multispectral Images. *Computers and Electronics in Agriculture*, 185-195.
- Maes, W., & Steppe, K. (2018). Perspective for Remote Sensing with Unmanned Aerial Vehicles in Precision Agriculture. *Trends in Plant Science*, 1-11.
- Munson, A. (1998). Nitrogen and Phosphorus Release from Humus and Mineral Soil under Black Spruce Forests in Central Quebec. *Soil Biology and Biochemistry*, 1491-1500.
- Pagola, M., Ortiz, R., Irigoyen, I., Bustince, H., Barrenechea, E., Aparicio-Tejo, P., . . . Lasa, B. (2009). New Method to Assess Barley Nitrogen Nutrition Status based on Image Colour Analysis Comparison with SPAD-502. *Computers and Electronics in Agriculture*, 213-218.
- Pölonen, I. (2013). Hyperspectral Imaging based Biomass and Nitrogen Content Estimations from Light-Weight UAV. *Proc. SPIE*.
- Rochester, I., Ceeney, S., Maas, S., Gordon, R., Hill, J., & Hanna, L. (2009). Monitoring Nitrogen Use Efficiency in Cotton Crops.
- Walsh, O. S., Shafian, S., Marshall, J., Jackson, C., Blanscet, S., Swoboda, K., . . . Walsh, W. (2018). Assessment of UAV-Based Vegetation Indices for Nitrogen Concentration estimation in Spring Wheat. *Advances in Remote Sensing*, 71-90.